

Experimental Comparison on Thermal Performance of Pulsating Heat Pipe and Embedded Heat Pipe Heat Spreaders

Sai Kiran Hota, Kuan-Lin Lee, Greg Hoeschele, Richard Bonner, Srujan Rokkam
Advanced Cooling Technologies, Inc.
1046 New Holland Building Ave 2,
Lancaster, PA, USA. 17601
saikiran.hota@1-act.com

Abstract

Two passive heat spreaders: one based on Embedded conventional Heat Pipes (EHP), and one based on internal capillary channel Pulsating Heat Pipes (PHP) were fabricated and tested for electronics cooling. The outer diameter of the heat pipes in the EHP was 5 mm, while the capillary channel diameter in the PHP was 1.6 mm. The PHP was charged with propylene up to 50% by volume. Experiments were performed at operating heat sink temperatures of -10 °C, 20 °C, and 40 °C with a stop condition of either dry-out or maximum heat spreader temperature exceeding 70 °C. At low heat sink temperatures, the thermal conductance of the PHP was comparable to the EHP. At higher heat sink temperatures of 20 °C and 40 °C, the thermal conductance of EHP was found to be significantly higher than the PHP. In the case of the PHP, dry-out was around 28.65 W/cm² at a low heat sink temperature of -10 °C, while no dry-out was observed in the EHP. When the heat sink temperature was 20 °C and 40 °C, dry-out occurred in the PHP at a heat flux of 23.65 W/cm² and 13.5 W/cm², respectively. EHP, on the other hand, did not show signs of dry-out at these heat sink temperatures. From experiments, it was determined that the thermal performance of the PHP was better than EHP at low to moderate heat flux until 19 W/cm² at a low heat sink temperature. At higher heat fluxes and heat sink temperatures, EHP showed higher thermal conductance than the PHP heat spreader at almost all heat fluxes.

Keywords

Heat spreader, thermal management, heat pipe, pulsating heat pipe, electronics cooling, two-phase cooling

Nomenclature

C	Thermal conductance (W/°C)
Q	Heat (W)
T	Temperature (°C)

1. Introduction

Performance advancements and rapid miniaturization of semiconductors have led to the development of high-power density power electronics systems. These improvements, however, impose high thermal heat flux challenges associated with decreasing efficiency and life [1]. The electronic chips, in general, must be maintained below 75 °C to maintain reliable operational performance [2]. Commonly employed electronics thermal management involves using a heat spreader to move high heat flux from electronics to a heat sink with a comparatively larger surface area. Existing commercial options usually use aluminum-based conduction plates for heat spreading. The performance of this conduction plate is limited by its material thermal conductivity and it may not be able to

handle high heat flux from high-power-density power electronics. So, for thermal management of high heat flux electronics, high thermal conductivity heat spreaders must be utilized.

Recently, two-phase heat transfer-based heat spreaders have been gaining attention as superior alternatives to conduction plates. An Embedded Heat Pipe (EHP) is one such solution that employs two-phase heat transfer mechanism of a heat pipe. Heat pipes have been investigated and well utilized for over 50 years [2]. In a heat pipe, the heat transfer is by vaporization of the working fluid in the heat receiving (evaporator) region and condensation of the vapor in the heat rejection (condenser) region [3]. Another solution involves two-phase heat transfer via the serpentine capillary channel in a heat spreader plate and is referred to as Pulsating Heat Pipe (PHP). PHP is a relatively newer passive thermal technology compared to heat pipes. In PHP, the heat transfer by means of pulsation of liquid slugs and vapor plugs driven by vapor pressure difference [4]. In the evaporator, the vapor pressure increases due to vaporization of the fluid, while in the condenser, the vapor pressure decreases due to shrinkage or condensation of the vapor bubble [4]. These continuous events result in pulsation of the working fluid.

Both EHP and PHP are passive thermal heat spreaders and have been investigated mostly independently. From the literature search, only one study was found comparing the thermal performance of the EHP and the PHP heat spreader-based electronics cooling system, but at a system level [5]. The study showed similar thermal performance between the EHP and the PHP-based cooling system. In this manuscript, the experimental performance of the two passive two-phase heat spreaders is presented and compared to identify the appropriate heat spreader for a given operating condition.

2. Heat spreader description and testing method

Flat plate EHP and PHP heat spreaders were fabricated with aluminum as the base material. The dimensions of the heat spreader are 160 mm x 233 mm x 3.56 mm, and conform to the standard 6U form factor of electronics cards as defined by VITA standards [6].

Figure 1 shows the mechanical specifications of the 6U form factor heat spreader. The PHP channel layout is specifically shown here since, in the finished product, the channels are inside the heat spreader. In the case of the EHP, the heat pipes are embedded into the base plate. The test configuration is also represented in Figure 1. A configuration with two center heating and edge heat rejection was chosen to simulate a central heat source and heat sink attachment on the edges. The heat source was a 25 mm x 25 mm heater block with

two cartridge heaters inserted. The heater blocks were fastened onto the heat spreader using threaded screws and bolts. For heat rejection, two cold plates were attached at the edges of the heat spreader. The width of the cold plate was 38 mm.

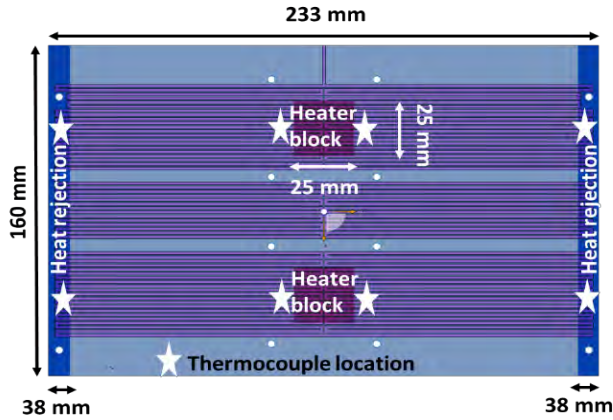


Figure 1. Mechanical specifications and test configuration of the heat spreaders (PHP channel layout is shown). Thermocouple locations are denoted with star markers

water heat pipes were chosen. The average length of the heat pipe was 222 mm and the diameter was 5 mm. Two wraps of copper screen mesh #100 was used as the wick. During fabrication process, slots of 3.35 mm thickness were made on the base plate and the heat pipe was flattened on the slots and soldered. In the case of the PHP, the diameter of the working fluid channels was 1.6 mm. Propylene was chosen as the working fluid since the PHP channel diameter conformed to the critical diameter dictated by the Bond number limit. Additionally, the PHP merit number [7] was found to be higher than other suitable working fluids. The other working fluid that was comparable to propylene was ammonia. The PHP was charged with propylene up to 50% of the volume. The thermo-physical properties of the fluid are listed in Table 1.

Table 1. Thermo-physical properties of EHP and PHP working fluids

	Water (EHP)		Propylene (PHP)	
	0	70	-10	70
Temperature (°C)				
Pressure (Pa)	6.11E2	3.12E4	4.29E5	3.09E6
Liquid density (kg/m ³)	1.00E3	9.78E2	5.59E2	4.04E2
Vapor density (kg/m ³)	4.80E-3	1.98E-1	9.15E0	7.70E0
Liquid viscosity (Pa.s)	1.80E-3	4.00E-4	1.15E-4	7.27E-5
Vapor viscosity (Pa.s)	9.22E-6	1.13E-5	7.74E-6	1.18E-5
Enthalpy of Vaporization (J/kg)	2.50E6	2.33E6	3.93E5	2.15E5
Surface tension (N/m)	7.57E-1	6.45E-2	1.17E-2	1.92E-3
Specific heat capacity of liquid (J/kg.K)	4.22E3	4.19E3	2.37E3	3.92E3

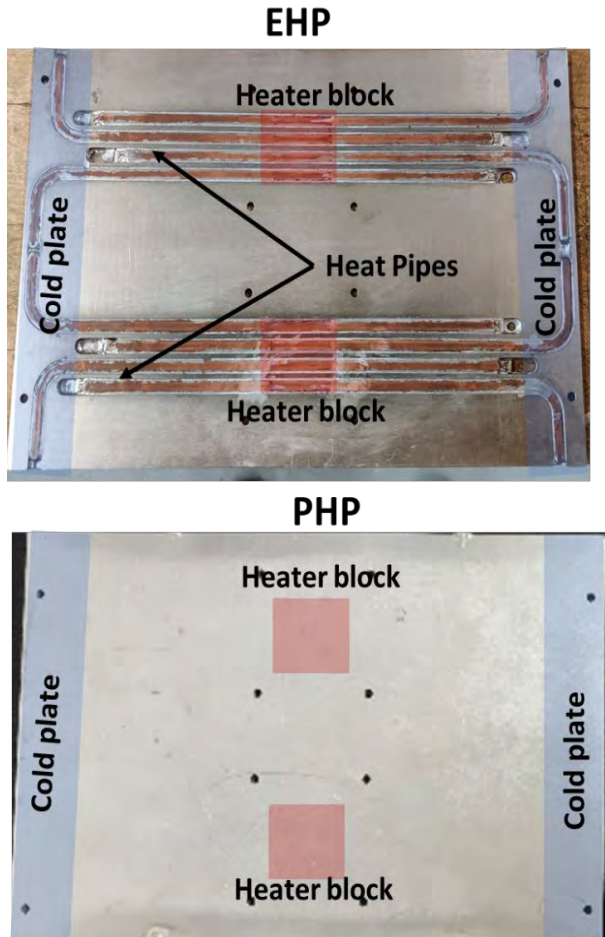


Figure 2. EHP and PHP heat spreaders

Figure 2 shows the EHP and PHP heat spreaders that were fabricated with an aluminum base plate. For EHP, 8 copper-

For performance testing of the heat spreaders, the Quasi-steady state testing method was adopted with incremental heater power. The heat spreader wall temperature at the heater section (evaporator) and the cold plate section (condenser) were recorded until a steady state was achieved for each given heater power. The testing was performed either until the maximum temperature on the heat spreader was 70 °C or dry-out occurred in the heat spreader. Dry-out condition is noted when the evaporator wall temperature increases sharply at a given heater power leading to a sudden decline in the thermal conductance of the heat spreader. The experimentally measured thermal conductance can be calculated as:

$$C = \frac{Q}{\Delta T} \quad (1)$$

Where 'Q' is the effective heater power and ' ΔT ' is the average temperature drop between the evaporator and the condenser. The thermocouple locations on the evaporator and the condenser are shown in Figure 1. Here the effective heater power is applied heater power divided by 4. This is due to the fact that there are two center evaporators and two edge condensers resulting four effective evaporator-condenser pairs. The heat spreaders were tested horizontal orientation with controlled cold plate surface temperature. The cold plate surface temperature will be referred to as heat sink temperature in this manuscript. During the performance testing, the coolant was supplied by a constant temperature chiller unit. Ethylene glycol (60% volume) was used as the coolant. The heat spreaders were insulated with standard 1" foam material to minimize heat leaks. Assuming an equivalent heat transfer coefficient of 5 W/m²-K, anticipated heat loss through insulation at heat spreader temperature of 70 °C is about 7.5 W.

3. Performance testing of the heat spreaders at various heat sink temperatures

The heat spreaders were tested at various operating heat sink temperatures of -10 °C, 20 °C, and 40 °C. The heat sink temperature here is the cold plate surface temperature. These temperatures were selected to represent heat sinks at low temperatures to moderately high temperatures existing in either terrestrial or space environments.

3.1. Baseline performance: Empty PHP plate

An empty PHP heat spreader was used to establish the baseline performance. The area cross-section of the solid material was 78.4% and overall solid volume fraction was ~ 84%.

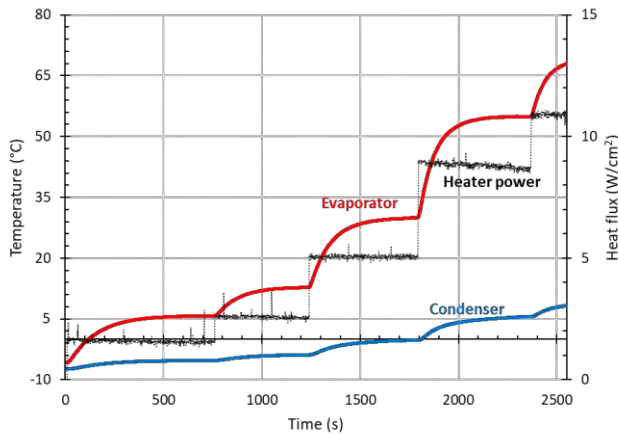


Figure 3. Wall evaporator and condenser temperatures of empty PHP heat spreader for baseline performance

Figure 3 shows the baseline evaporator (red) and condenser (blue) wall temperatures of the empty PHP heat spreader with increasing heat flux. The cold plate surface temperature was maintained at -10 °C. During the tests, it was noticed that the sink temperature increased at moderately higher heat flux (> 10 W/cm²), possibly due to smaller heat rejection area and also due to limited heat removal capacity of the constant temperature fluid bath. At maximum heat flux of ~10.3 W/cm², the cold plate temperature increased to 0.5 °C.

The temperatures increase proportionally with the applied heat flux. The maximum heat spreader temperature was 67.8 °C when the heat flux was 10.3 W/cm². Estimated percentage heat lost through the insulation was ~ 5.4% for conduction plate.

Similarly, quasi-steady state testing of the baseline empty PHP heat spreader was performed at other heat sink temperatures of interest. Similar proportional increase in the evaporator and the condenser temperatures were observed with increasing heat flux. The maximum heat flux at 20 °C and 40 °C operating conditions was ~13.5 W/cm² and ~7 W/cm², respectively. The maximum recorded heat spreader temperature was between 65 to 70 °C.

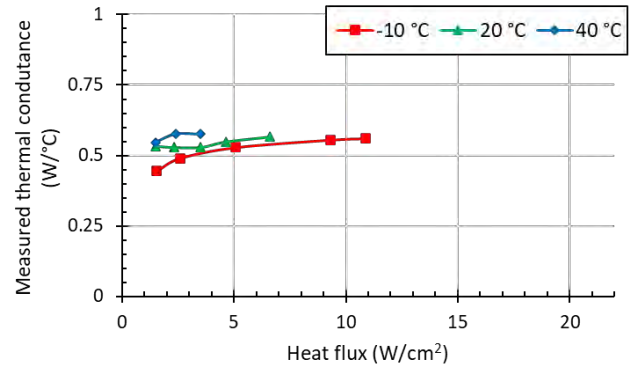


Figure 4. Thermal conductance of the empty PHP heat spreader

The experimental thermal conductance of the conduction plate heat spreader was determined using eq. 1. Figure 4 shows the thermal conductance of the conduction plate heat spreader with varying heat fluxes at different operating cold plate (sink) temperatures. The average measured thermal conductance of the heat spreader was 0.54 W/°C with an uncertainty of 0.04 W/°C. Accounting for the solid area fraction of 78.4%, the apparent thermal conductance of solid conduction plate was estimated to be 0.69 W/°C.

3.2. Two Phase Heat Spreader Performance

Testing at heat sink temperature of -10 °C

The EHP and the PHP heat spreaders were tested at a cold plate temperature of -10 °C. The wall temperature measurements at incremental heater powers are shown in Figure 5. The wall evaporator and condenser temperature increased with increasing heater power. Compared to baseline results, it was observed that the increase in the temperature difference between the evaporator and the condenser was not proportional to the heater power meaning that the thermal conductance varied with the heater power. The EHP heat spreader did not dry out and the maximum heat spreader temperature of ~68.7 °C occurred at an applied heat flux of ~42.2 W/cm². However, in the case of the PHP, dry-out occurred when the applied heat flux increased from 50 W/cm² to 28.5 W/cm². So, the maximum heat flux with PHP is between 25 to 28.5 W/cm².

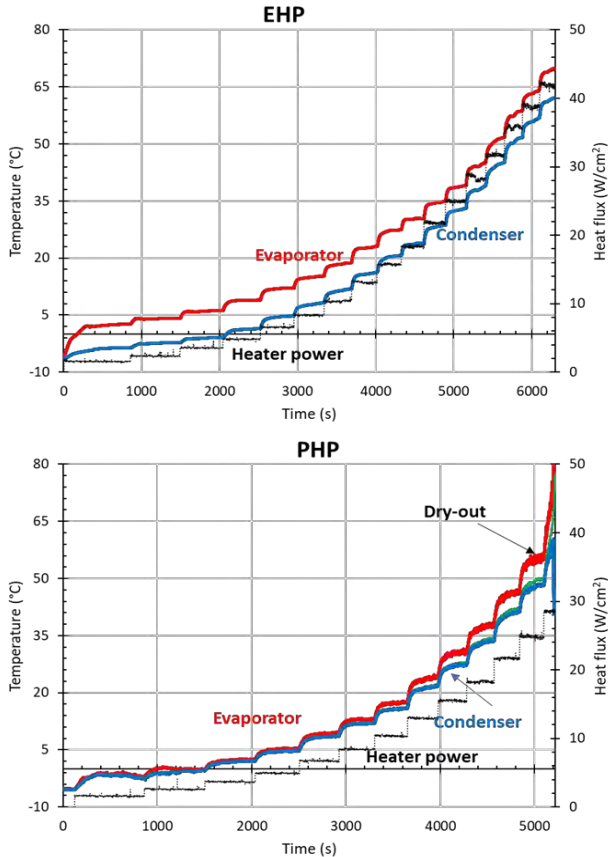


Figure 5. Wall evaporator and condenser temperatures of the EHP and the PHP heat spreaders at heat sink temperature of $-10\text{ }^{\circ}\text{C}$

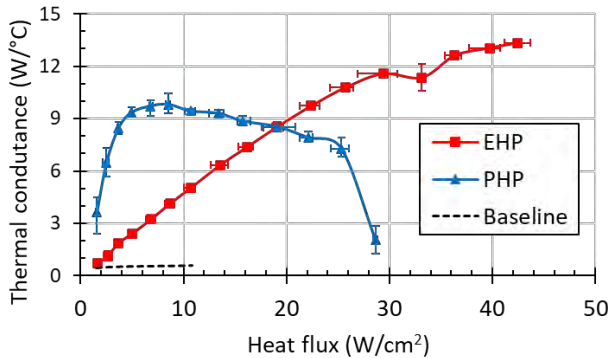


Figure 6. Thermal conductance of the EHP and PHP heat spreaders at heat sink temperature of $-10\text{ }^{\circ}\text{C}$

The thermal conductance of the EHP and the PHP is shown in Figure 6. The thermal conductance increased with increasing heat flux for both the heat spreaders. The thermal conductance of the PHP increased from above $3\text{ W}/^{\circ}\text{C}$ at a heat flux of $1.55\text{ W}/\text{cm}^2$ to more than $9\text{ W}/^{\circ}\text{C}$ at a heat flux of $5\text{ W}/\text{cm}^2$. The thermal conductance of the PHP stayed above $9\text{ W}/^{\circ}\text{C}$ until the heat flux of $13.4\text{ W}/\text{cm}^2$, after which, the thermal conductance was reduced. The thermal conductance of the EHP, on the other hand, showed an increasing trend with increasing heat flux. However, as the heat flux increased, the mean EHP temperature increased and an improvement in the performance was

observed. The thermal conductance of the EHP was lower than the PHP until the heat flux of $19\text{ W}/\text{cm}^2$. Above this heat load, the EHP showed higher thermal conductance, while the PHP showed a declining trend in thermal conductance.

Testing at heat sink temperature of $20\text{ }^{\circ}\text{C}$

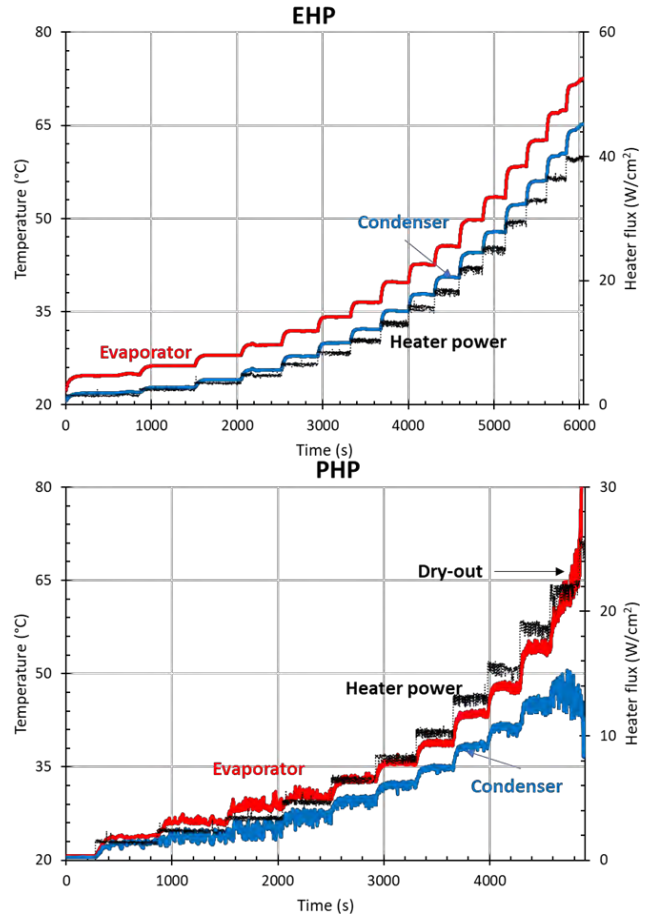


Figure 7. Wall evaporator and condenser temperatures of the EHP and the PHP heat spreaders at heat sink temperature of $-10\text{ }^{\circ}\text{C}$

The EHP and the PHP heat spreaders were then tested with the heat sink at $20\text{ }^{\circ}\text{C}$. Quasi-steady state temperature profiles of the heat spreaders are shown in Figure 7. The wall temperatures increase with increasing heat flux, similar to the tests performed at lower heat sink temperatures. The EHP evaporator temperature was $\sim 72\text{ }^{\circ}\text{C}$ at the heat flux of $39\text{ W}/\text{cm}^2$. No dry-out was observed. In the case of the PHP, when the heat increased from $18.75\text{ W}/\text{cm}^2$ to $21.15\text{ W}/\text{cm}^2$, the condenser temperature increased but the evaporator temperature continued to increase, indicating partial dry-out operation. When applied heat flux increased to $25.1\text{ W}/\text{cm}^2$, dry-out occurred in the PHP with rapidly increasing evaporator temperature and rapidly decreasing condenser temperature. The evaporator wall temperature of the PHP was $65\text{ }^{\circ}\text{C}$ when dry-out was observed.

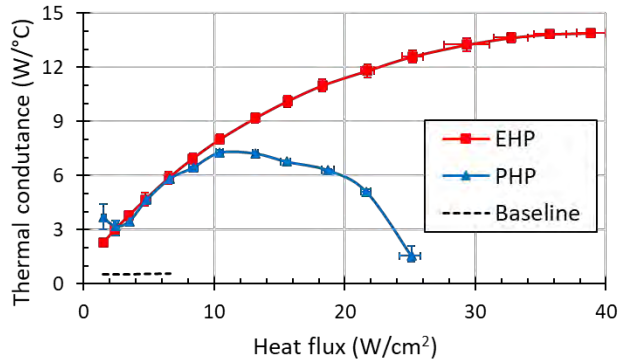


Figure 8. Thermal conductance of the EHP and PHP heat spreaders heat sink temperature of 20 °C

Figure 8 shows the thermal conductance of the EHP and the PHP heat spreaders at the heat sink temperature of 20 °C. The thermal conductance of the EHP increased with increasing heat flux, while for the PHP, the thermal conductance increased to a certain value and then declined. At a low heat flux of 1.5 W/cm², the thermal conductance of the PHP was 3.67 W/°C, which was higher than the EHP at 2.26 W/°C. As heat flux increased up to 6.6 W/cm², the thermal conductance of both EHP and the PHP was found to be similar to one another. The thermal conductance of the EHP and the PHP was 5.86 W/°C and 5.83 W/°C, respectively. The thermal conductance of the EHP continuously increased to a value of 13.8 W/°C at 35.75 W/cm². In the case of the PHP, the maximum thermal conductance of 6.8 W/°C was obtained at the heat flux of 15 W/cm², which was reduced to 6.3 W/°C at a heat flux of 18.7 W/cm². Further increasing the heat flux, first resulted in partial dry-out at 21.1 W/cm² with thermal conductance of 5.1 W/°C, then full dry-out at 25.1 W/cm².

Testing at heat sink temperature of 40 °C

The heat spreaders were further tested at a heat sink temperature of 40 °C. Quasi-steady state temperature profiles of the heat spreaders are shown in Figure 9. The wall temperatures increased with increasing heat flux in both the heat spreaders as anticipated. The EHP evaporator temperature was ~ 72 °C at a heat flux of 20.35 W/cm². No dry-out was observed. In the case of the PHP, dry-out was observed when the applied heat flux was ~ 12.5 W/cm². This test shows that the EHP operates at a higher heat flux than the propylene PHP at a higher heat sink temperature. The wall temperature fluctuation in the PHP at this heat sink temperature was also noted to be more vigorous than at lower temperatures. At elevated operating conditions, PHP pulsates more vigorously because of very high dP/dT, lowering surface tension and other thermo-physical properties of the fluid which increases the frequency of pulsation. When the heat flux increases from 10 W/cm² to 12.5 W/cm², dry-out occurs in the PHP.

Figure 10 shows the thermal conductance of the EHP and the PHP heat spreaders at a heat sink temperature of 40 °C. The thermal conductance of the EHP showed an increasing trend with the heat flux, similar to the performance testing at lower

heat sink temperatures. However, on the other hand, the thermal conductance of the PHP showed a declining trend with the increasing heat flux. The error margin across other tests performed at the same heat sink temperature was relatively higher than at lower heat sink temperature, indicating relatively less reliability of the (propylene charged) PHP at high heat sink temperature. The performance of the EHP stayed consistent across all tests performed at this heat sink temperature.

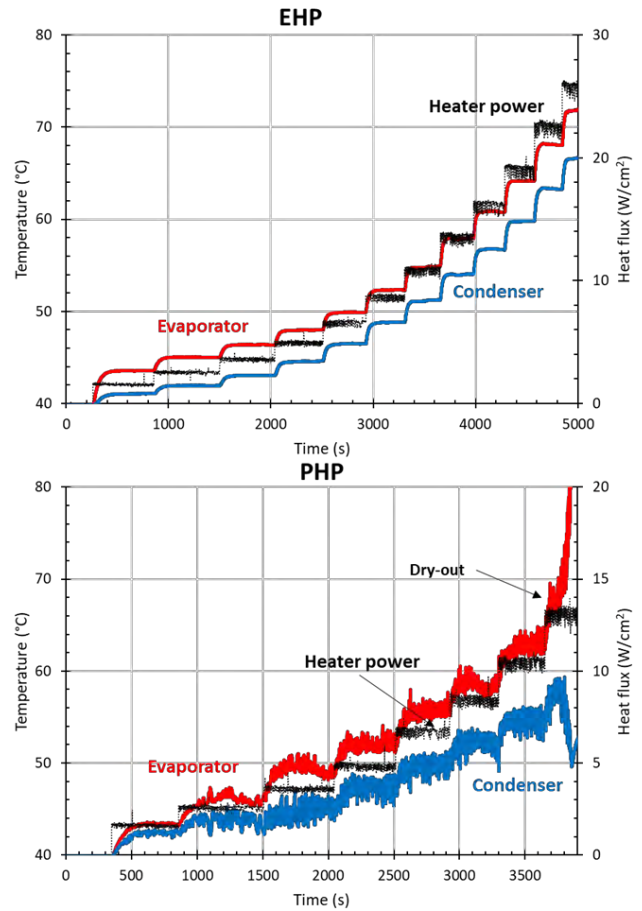


Figure 9. Wall evaporator and condenser temperatures of the EHP and the PHP heat spreaders at heat sink temperature of 40 °C

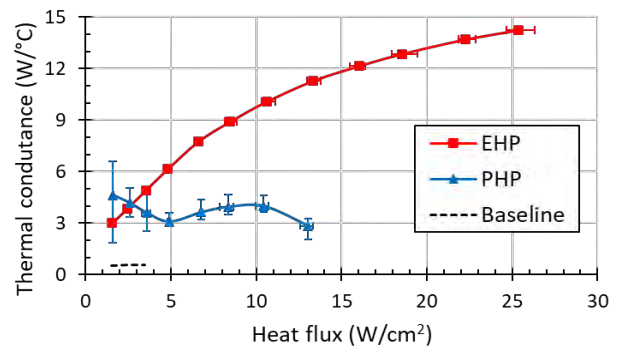


Figure 10. Thermal conductance of the EHP and PHP heat spreaders heat sink temperature of 40 °C

3.3. Thermal conductance comparison of the heat spreaders

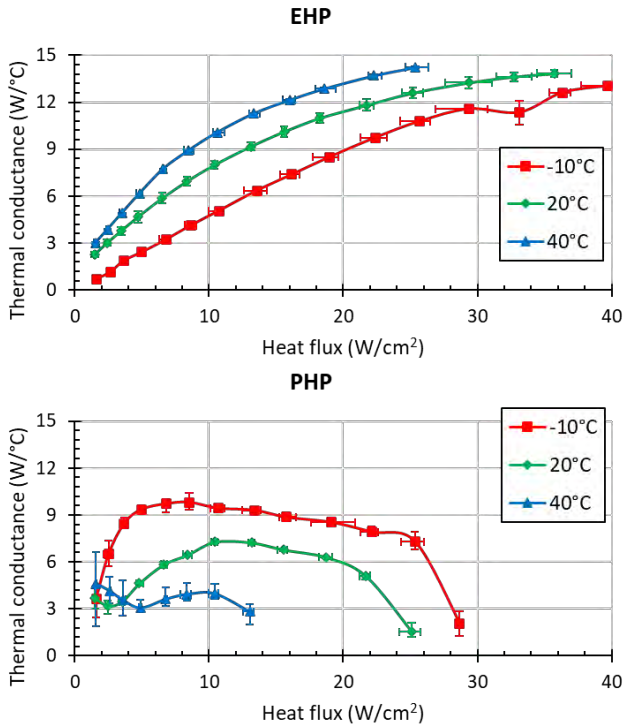


Figure 11. Thermal conductance of EHP and PHP with varying heat sink temperatures

Thermal performance of the EHP and PHP with varying heat sink temperatures is shown in Figure 11. Opposing trends of thermal conductance were observed with the EHP and the PHP. At low heat flux of 1.5 W/cm^2 , the thermal conductance of the EHP was only $0.71 \text{ W/}^\circ\text{C}$, while at a higher heat sink temperature of 20°C and 40°C , the thermal conductance was $2.26 \text{ W/}^\circ\text{C}$ and $3 \text{ W/}^\circ\text{C}$, respectively. As the heat flux increases, the thermal conductance increases in the EHP. When the heat flux was $\sim 25 \text{ W/cm}^2$, $10.8 \text{ W/}^\circ\text{C}$ at a heat sink temperature of -10°C , while at 20°C and 40°C heat sink temperatures, the thermal conductance of the EHP was $12.6 \text{ W/}^\circ\text{C}$ and $14.2 \text{ W/}^\circ\text{C}$, respectively. However, in the case of PHP, a different trend is observed. In general, at a given heat flux, the thermal conductance was lower with increasing heat sink temperature, indicating that the (propylene-charged) PHP is more suitable at lower heat sink temperatures. At a heat sink temperature of -10°C and 20°C , the thermal conductance first increases with increasing heat flux and reaches the maximum. Further increasing the heat flux then results in the reduction of the thermal conductance until dry-out occurs, at which point, the thermal conductance sharply decreases.

3.4. Heat transfer operating limits of the PHP

From the comparison performance testing, it was determined that the EHP operates without dry-out, while, dry-out occurs in the PHP. Tests were performed at elevated heat fluxes to determine the maximum heat transfer operating limit of the PHP.

Figure 12 shows the maximum operating heat flux condition and temperature at PHP dry-out. When the sink temperature is -10°C , the dry-out occurs in the PHP at 28.65 W/cm^2 . Increasing the heat sink temperature reduces the maximum heat flux-carrying capability of the PHP. At 20°C heat sink temperature, the dry-out occurred when the applied heat flux was 23.65 W/cm^2 . Further increasing the heat sink temperature to 40°C resulted in a sharp reduction in the dry-out flux, which was 13.5 W/cm^2 . Corresponding maximum wall evaporator temperatures just before the dry-out were 54.5°C , 65.6°C , and 71.5°C , respectively.

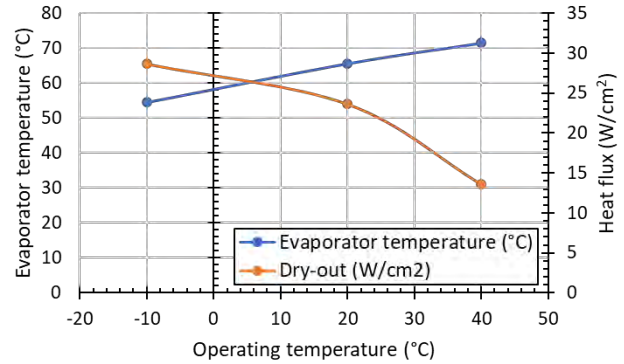


Figure 12. Maximum heat flux capability and maximum temperature of the propylene charged PHP before dry-out

4. Conclusions

Experimental performance comparison of two two-phase passive heat spreaders, the embedded heat pipe (EHP) and the pulsating heat pipe (PHP) are presented here. The dimensions of the heat spreader were $233 \text{ mm} \times 160 \text{ mm} \times 3.56 \text{ mm}$, which conforms to the standard 6U form factor electronics heat spreader as defined by the VITA standards. The EHP heat spreader consisted of 8 copper-water heat pipes embedded into an aluminum base plate. The PHP was charged with propylene as the working fluid up to 50% by volume. Quasi-steady state performance testing was done on the heat spreaders to determine and compare the performance at heat sink temperatures: -10°C , 20°C , and 40°C , respectively. The testing was stopped when either dry-out occurred or when the maximum temperature of the heat spreader was 70°C .

From the performance testing of the heat spreaders, the following conclusions are drawn:

- At a lower heat sink temperature of -10°C , the thermal conductance of the PHP was higher than the EHP at heat fluxes lower than 19 W/cm^2 . When the heat flux was higher than 38 W/cm^2 , the thermal conductance of the EHP dominated the thermal conductance of the PHP. The maximum heat flux transported by the EHP and the PHP before the stop condition was 42.5 W/cm^2 , and 25.35 W/cm^2 , respectively. The improvement over the conventional conduction heat spreader with a maximum heat flux of 10.35 W/cm^2 was 3.94 times and 2.33 times, respectively with EHP and the PHP heat spreaders.
- At a heat sink temperature of 20°C , the thermal conductance of both the EHP and the PHP were comparable until the heat flux of 6.6 W/cm^2 . Further increasing the heat flux showed that the thermal conductance of the EHP was higher than the PHP. The maximum heat flux transported by

the EHP and the PHP before the stop condition was little lower than 39 W/cm^2 , and 23.65 W/cm^2 , respectively. The improvement over the conventional conduction heat spreader with a maximum heat flux of 6.75 W/cm^2 was 5.78 times and 3.5 times, respectively with EHP and the PHP heat spreaders.

- At a higher heat sink temperature of $40 \text{ }^\circ\text{C}$, the thermal conductance of the EHP was found to be higher than the PHP. The maximum heat flux transported by the EHP and the PHP before the stop condition was little lower than 25.35 W/cm^2 , and 13.55 W/cm^2 , respectively. The improvement over the conventional conduction heat spreader with a maximum heat flux of 7 W/cm^2 was 7.24 times and 3.87 times, respectively with EHP and the PHP heat spreaders.

- The variation of the thermal conductance of the EHP and the PHP showed opposing trends with heat sink temperature. At a given heat flux, the thermal conductance of the EHP was higher at a higher heat sink temperature. The thermal conductance trend of the PHP showed an opposing trend with a lower value at a higher heat flux.

No dry-out was observed in the case of the EHP. However, in the PHP, dry-out occurred in all three cases. When the heat sink temperature was $-10 \text{ }^\circ\text{C}$, the dry-out occurred at a heat flux of 28.65 W/cm^2 . The maximum heat flux decreased with increasing heat sink temperature in the PHP. When the heat sink temperature was $20 \text{ }^\circ\text{C}$ and $40 \text{ }^\circ\text{C}$, dry-out occurred in the PHP at a heat flux of 23.65 W/cm^2 and 13.55 W/cm^2 , respectively.

Acknowledgments

This work was initiated as ACT's internal R&D project and was continued with the support of NASA's Small Business Innovation Research (SBIR) Phase II contract #80NSSC22CA205. The authors are grateful to Dr. Jeffrey R. Didion for his support. The authors express their gratitude to engineering technicians, Mr. Eugene Sweigart and Mr. Samuel Martzall for their support with fabrication and experiments. The authors also thank Mr. Tim Wagner for his support with welding tasks.

References

1. Y.-G. Lv, W.-X. Chu and Q.-W. Wang, "Thermal management systems for electronics using in deep downhole environment: A review," *International Communications in Heat and Mass Transfer*, vol. 139, page. 106450, 2022.
2. S. M. S. Murshed and C. A. N. de Castro, "A critical review of traditional and emerging techniques and fluids for electronics cooling," *Renewable and Sustainable Energy Reviews*, vol. 78, page. 821-833, 2017.
3. <https://www.1-act.com/resources/heat-pipe-resources/faq/#:~:text=What%20is%20a%20Heat%20Pipe,in%20an%20extremely%20efficient%20way.>
4. Vadim S. Nikolayev and M. Marengo, "Pulsating Heat Pipes: Basics of Functioning and Modeling", in: *Encyclopedia of Two-Phase Heat Transfer and Flow IV*. page. 63-139, 2018.
5. K.-L. Lee, S.K. Hota, A. Lutz, and S. Rokkam, "Advanced Two-Phase Cooling System for Modular Power Electronics", 51st International Conference on Environmental Systems, 2021.
6. ANSI/VITA 48.2-2020, "Mechanical Standard for VPX REDI Conduction Cooling". VITA© 2021.

7. J. Kim and S.J. Kim, "Experimental investigation on working fluid selection in a micro pulsating heat pipe", *Energy Conversion and Management*, vol. 205, page. 112462, 2020.